UCRL-ID-130064 Rev 1

Waste Package Degradation Expert Elicitation Panel: Input on the Corrosion of CRM Alloy C-22

Joseph C. Farmer

February 26, 1998

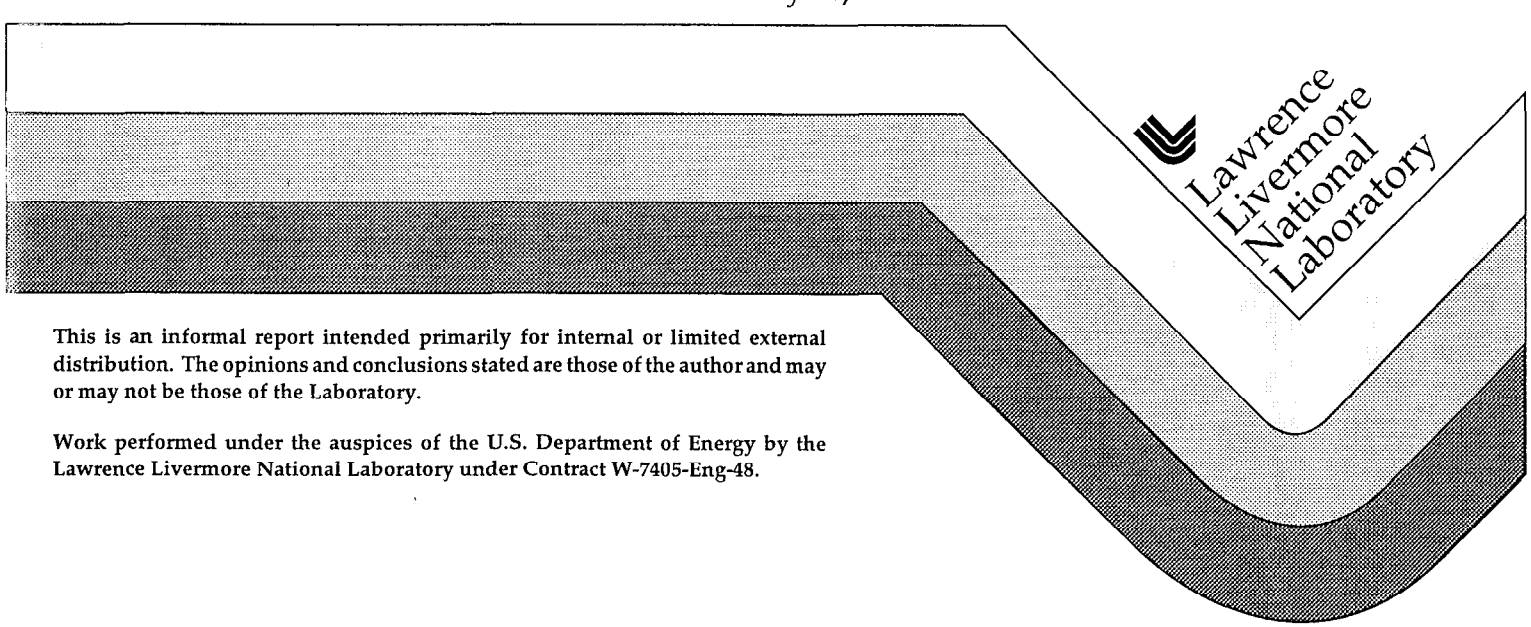

Work performed under the auspices of the U.S. Department of Energy by the Lawrence Livermore National Laboratory under Contract W-7405-Eng-48.

WASTE PACKAGE DEGRADATION EXPERT ELICITATION PANEL: INPUT ON THE CORROSION OF CRM ALLOY C-22

Joseph C. Farmer
University of California
Lawrence Livermore National Laboratory
7000 East Avenue or P.O. Box 808
Livermore, California 94550
Telephone 510-423-6574
Fax 510-423-2086
Secretary 510-422-9279 (Nan Poggio)

February 26, 1998 – First Version

ANTICIPATED ENVIRONMENTS

The overall electrolyte concentration in the NFE environment is expected to be somewhere between 1X and saturated J-13 well water. This covers more than three orders-of-magnitude in chloride anion concentration. The pH of this solution is expected to be somewhere between 5 and 10. Exposed patches of the CRM could see this environment.

The pH in the crevice can be acidified due to the hydrolysis of dissolved polyvalent cations, such as Fe^{2+}. As discussed by Oldfield and Sutton, metal ions produced by anodic dissolution are assumed to undergo the following hydrolysis reactions [J. W. Oldfield, W. H. Sutton, "Crevice Corrosion of Stainless Steels: I. A Mathematical Model," British Corrosion Journal, Vol. 13, No. 1, 1978, pp. 13-22]:

$$Fe^{2+} + H_2O \underset{K_{31}}{\longleftrightarrow} Fe(OH)^{+} + H^{+}$$

$$Fe^{3+} + H_2O \underset{K_{41}}{\longleftrightarrow} Fe(OH)^{2+} + H^{+}$$

$$Ni^{2+} + H_2O \underset{K_{51}}{\longleftrightarrow} Ni(OH)^{+} + H^{+}$$

$$Cr^{3+} + H_2O \underset{K_{11}}{\longleftrightarrow} Cr(OH)^{2+} + H^{+}$$

$$Cr(OH)^{2+} + H_2O \underset{K_{12}}{\longleftrightarrow} Cr(OH)_2^{+} + H^{+}$$

These reactions have also been considered in a crevice corrosion model published by the NRC [J. C. Walton, S. K. Kalandros, "TWITCH – A Model for Transient Diffusion, Electromigration, and Chemical Reaction in One Dimension," Center for Nuclear Waste Regulatory Analyses, San Antonio, TX, CNWRA 92-019, 1992]. The range of pH expected under a worst-case scenario (no precipitation of $FeCO_3$; no leakage of dissolved metal or acid out of the crevice; no pH buffers; etc.) is illustrated by the data of Jones et al., as shown in Table 1 [D. A. Jones, B. E. Wilde, "Galvanic Reactions During Localized Corrosion on Stainless Steel," Corrosion Science, Vol. 18, 1978, pp. 631-643].

Table 1. Suppression of pH by Hydrolysis Reactions in $FeCl_2$, $NiCl_2$, and $CrCl_3$ (25 °C).

Salt	1 N	3 N	Saturated
$FeCl_2$	2.1	0.8	0.2
$NiCl_2$	3.0	2.7	2.7
$CrCl_3$	1.1	-0.3	-1.4

The lowest possible pH values expected with $FeCl_2$ solutions at 25°C is 0.2. The pH levels measured in $FeCl_3$ solutions by Francis Wang are shown in Table 2.

Table 2. Suppression of pH by Hydrolysis Reactions in $FeCl_3$ Solutions (25 °C).

$FeCl_3$ (wt. %)	pH
1	1.92
2	1.83
3	1.71
4	1.63
10	0.70

More realistic estimates must include transport of Fe^{2+} and other species out of the crevice, limitations on the rate of Cl^- transport into the crevice, pH buffer effects due to other ion, and precipitation of hydrolyzable Fe^{2+} by carbonate. Such effects will tend to make the pH higher than these extreme values based upon thermodynamic equilibrium. A transport model for crevice corrosion has been developed by two of members of this Expert Elicitation Panel and was used to predict a pH of roughly 2.8-3.2 during the attack of Alloy 625 [J. C. Farmer, R. D. McCright, "Crevice Corrosion and Pitting of High-Level Waste Containers: Integration of Deterministic and Probabilistic Models," Paper No. 160, Annual Meeting of the National Association of Corrosion Engineers (NACE), Corrosion 98, San Diego, CA March 22-27, 1998].

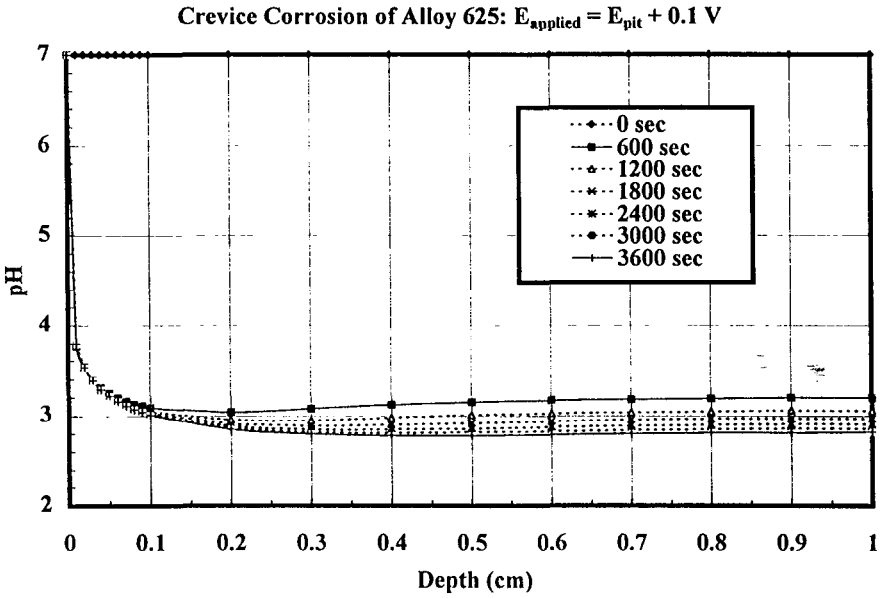

Figure 1. Prediction of transport-limited pH suppresion in crevice during attack of Alloy 625. The potential assumed as a boundary condition at the crevice mouth (applied potential) was fixed at a level 100 mV more anodic that the critical pitting potential of Alloy 625.

During the Appendix 7 Meeting, the range of expected values given by the NRC Center are:

A. NFE $5 < pH < 10$

B. Crevice - Before Localized Corrosion of CRM: $3 < pH < 5$. Likely case, since this will occur near Ecorr of A516. Due to hydrolysis of Fe alone. Depends upon transport and crevice geometry.

C. Crevice - After Localized Corrosion of CRM: $-1 < pH < 3$. Requires potential above repassivation potential, and considered very unlikely. Due to hydrolysis of other dissolved metals, such as Cr and Mo. Depends on transport and crevice geometry.

It is believed that the electrochemical potential at the mouth of the crevice will be somewhere between the mixed potential of A516 Gr 12 and Alloy C-22, in either concentrated J-13 or concentrated (10 wt. % $FeCl_3$). See Table 3.

Table 3. Expected Electrochemical Potentials in Repository – Based on Measurements of A516 Gr. 12 (CAM) and Alloy C-22 (CRM).

Case	A	B	C	D	E
T (°C)	90	90	90	90	90
NaCl (wt. %)	10	1	0	0	5
$FeCl_3$ (wt. %)	0	0	0.6	3.1	0
pH	6.8	2.7	2.14	1.72	2.7
Radiolysis	No	No	No	No	No
Deaerated	No	Yes	Yes	Yes	No
E_{corr} (mV vs. SHE): A516 Gr 12					-520
E_{corr} (mV vs. SHE): C-22	-24	-29	+661	+714	
E_{pit} (mV vs. SHE): C-22	+442	+758	+905	+889	> +730
E_{pass} (mV vs. SHE): C-22	+550	+793	+857	+896	> +730
Above Threshold Potential	No	No	No	No	No

In the absence of $FeCl_3$, which is a product of the CAM corrosion, the greatest mixed potential expected is somewhere between –520 and –29 mV vs. SHE at 90°C. With $FeCl_3$ at 10 wt. %, potentials as high as +714 mV vs. SHE have been observed. Since the observed mixed potential never exceeded the pitting potential or the repassivation potential, localized attack is not be expected. This interpretation is consistent with the interpretation of Cragnolino [G. A. Cragnolino, DOE/NRC Appendix 7 Meeting, Livermore, CA, February, 1998]. These observations do not account for the effects of gamma radiolysis and other effects.

From transport modeling of corrosion in the CAM-CRM crevice, it is known that the electrochemical potential inside the crevice is less anodic (less severe) than the potential established or applied at the mouth of the crevice [J. C. Farmer, R. D. McCright, "Crevice Corrosion and Pitting of High-Level Waste Containers: Integration of Deterministic and Probabilistic Models," Paper No. 160, Annual Meeting of the National Association of Corrosion Engineers (NACE), Corrosion 98, San Diego, CA March 22-27, 1998]. This is due to ohmic drop along the length of the crevice. Consequently, any estimate of corrosion rate based on the electrochemical potential at the crevice mouth, coupled with the assumption of suppressed pH and elevated chloride inside the crevice, should be conservative.

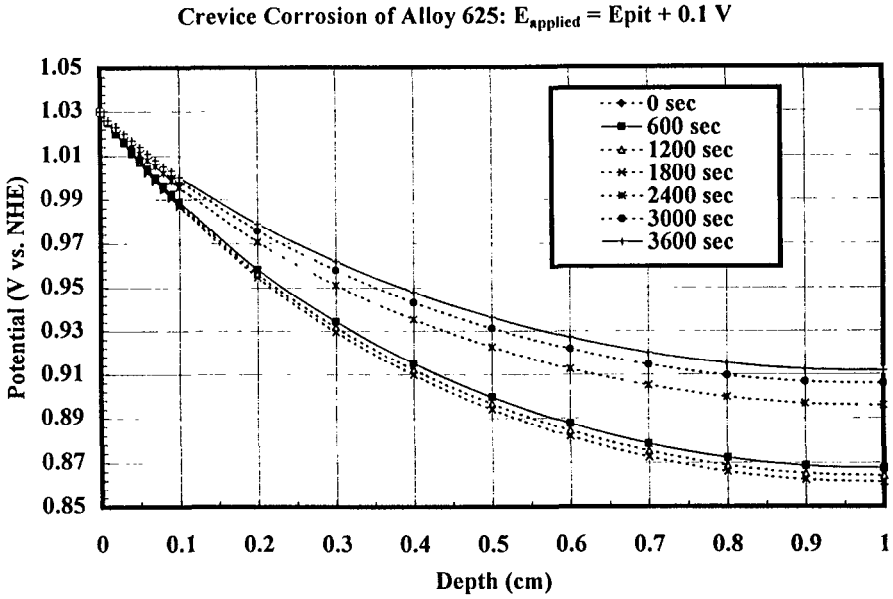

Figure 2. Electrochemical potential inside crevice is less severe than that applied in the mouth. The potential assumed as a boundary condition at the crevice mouth (applied potential) was fixed at a level 100 mV more anodic that the critical pitting potential of Alloy 625. Corresponds to Figure 1.

In summary, the environmental conditions determined to be of greatest interest by consensus of the entire Expert Elicitation Panel are summarized below:

A. Temperature: T = 25, 50, and 100°C

B. Acidity: pH = 2.5 & 3-10

C. Electrochemical Potential: E = 340 & 640 mV vs. SHE

PASSIVE CORROSION RATES OF ALLOY C-22 IN RELEVANT ENVIRONMENTS

Questions:

1) What is the general corrosion (or passive dissolution) rate of the C-22 inner barrier in humid-air conditions (i.e., without drips) at 25, 50 and 100°C?

It is assumed that without drips, the inner barrier is exposed to mostly benign conditions in the potential repository.

The corrosion rates given should specify, as a minimum, the 0th and 100th percentile values along with the median, 5th percentile and 95th percentile values.

2) What is the general corrosion (or passive dissolution) rate of the inner barrier under dripping conditions?

Please consider the combination of temperature, pH 7-10, and concentrated chemistry conditions represented by 1000X J-13 and fully saturated J-13:

The corrosion rates given should specify, as a minimum, the 0th and 100th percentile values along with the median, 5th percentile and 95th percentile values.

Response:

Reasonable values for the penetration rate of Alloy C-22 due to dissolution through the passive film appear to be between 0.009 microns per year in a simulated, acidified, concentrated, J-13 well water, and 13 microns per year in a simulated crevice solution. Passive corrosion is consistent with opinions voiced by representative of the NRC. They state that no significant localized corrosion (localized penetration of the passive film) occurs at potentials well below the repassivation potential, E_{pass}. In the absence of radiolysis, the measured corrosion potential (mixed potential), E_{corr}, in such environments appears to be well below E_{pass}. This is a general view held by other investigators in the field of corrosion science. The observed penetration rates for Alloy C-22 in relevant environments are summarized in Figure 3, and are indicative of passive corrosion.

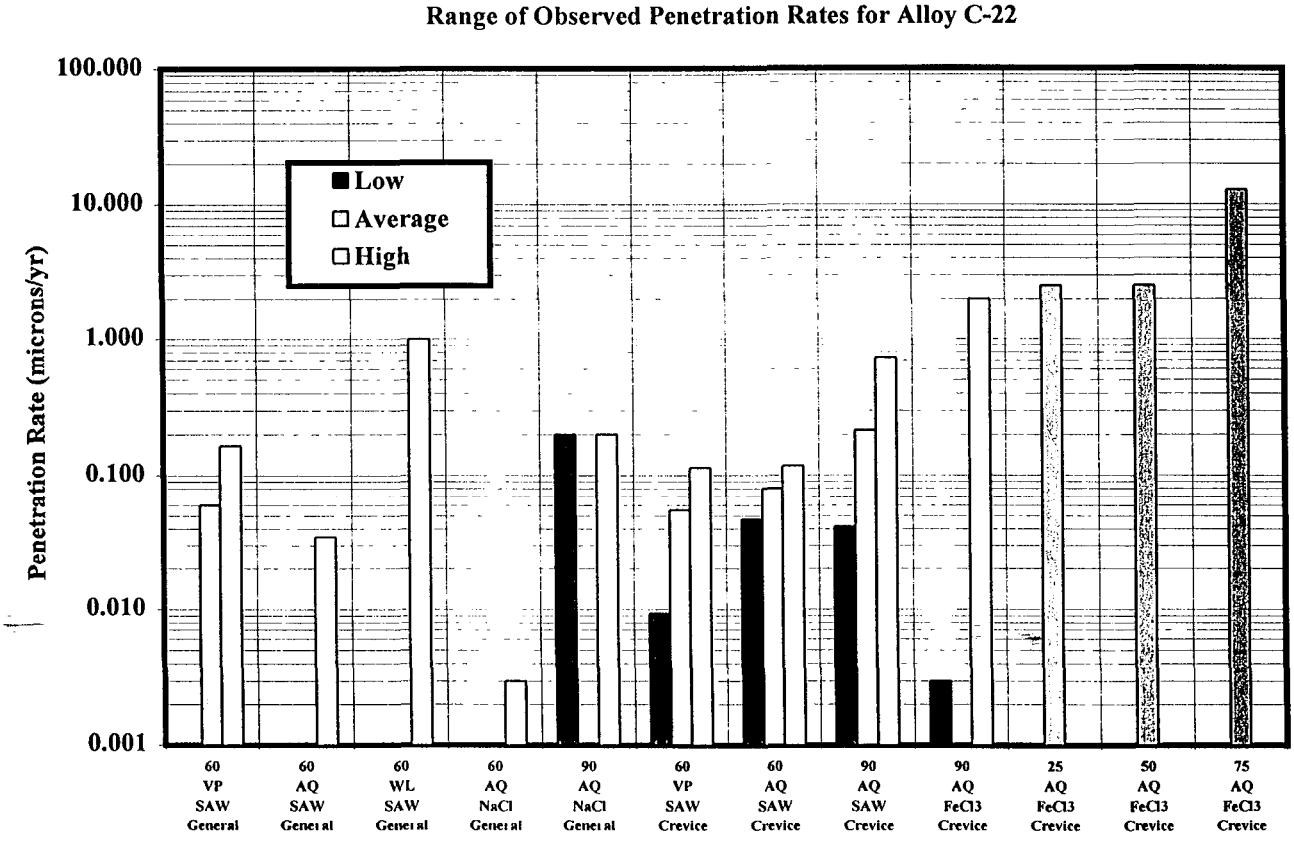

Figure 3. Observed Passive Corrosion Rates for Alloy C-22: Measured Weight Loss of Samples Exposed in Long Term Corrosion Test Facility (LTCTF); Corrosion Current Measurements at Open Circuit Potential (Roy, LLNL); and Measured Weight Loss of Samples Exposed to Simulated Crevice Solutions (Asphahani, Hanes International).

These observations are well represented by the regression equation (correlation) given to the EEP earlier. Data from the LTCTF was combined with the rates calculated from Roy's linear sweep polarization measurements, as well as the rates published by Asphahani. The combined data set was then used as the basis of an overall correlation of penetration rates with temperature, pH, equivalent NaCl concentration, and $FeCl_3$ [J. C. Farmer et al., "Development of Models for High-Level Waste Containers," Proc. 6th Intl. Conf. On Nuclear Engineering, ICONE-6, May 10-15, 1998, San Diego,

California, ASME, 1998, 13 p.]. The following linear equation was found to be adequate for the correlation of Alloy C-22 penetration rates:

$$\ln\left(\frac{\Delta p}{\Delta t}\right) = b_0 + b_1\left(\frac{1000}{T+273}\right) + b_2(pH) + b_3(C_{NaCl}) + b_4(C_{FeCl_3})$$

where $\Delta p/\Delta t$ is the apparent penetration rate ($\mu m\ y^{-1}$); T is the temperature (°C); C_{NaCl} is the equivalent concentration of NaCl (wt. %); and C_{FeCl3} is the concentration of $FeCl_3$ (wt. %). Within the bounds of thirty-eight (38) experimental observations for Alloy C-22, the coefficients were determined to be:

$b_0 = +13.409$
$b_1 = -5.5587$
$b_2 = -0.87409$
$b_3 = +0.56965$
$b_4 = +0.60801$

More specifically, the correlation for Alloy C-22 is:

$$\ln\left(\frac{\Delta p}{\Delta t}\right) = 13.409 - \left(\frac{5558.7}{T+273}\right) - 0.87409(pH) + 0.56965(C_{NaCl}) + 0.60801(C_{FeCl_3})$$

The "standard error of estimate" ($s_{y/1234}$) and the "sample multiple variable regression coefficient" ($r_{y/1234}$) are defined by Crow, Davis and Maxfield [E. L. Crow, F. A. Davis, M. W. Maxfield, Statistics Manual, Dover Publications, Inc., New York, NY, 1960, pp. 147-19]. The "standard error of estimate" is a measure of the scatter of the observed penetration rates about the regression plane. About 95% of the points in a large sample are expected to lie within $\pm 2s_{y/123\ k}$ of the plane, measured in the *y* direction. Values for the above correlation are:

$s_{y/1234} = 1.5092$
$r_{y/1234} = 0.65628$

The "multiple variable regression coefficient" indicates a reasonably good fit to the data set, given the large number of independent variables. As discussed in the literature, uncertainty in a given model parameter, β_j, can be determined from the standard error of estimate, as shown by Eqns. 7 and 8 [E. L. Crow, F. A. Davis, M. W. Maxfield, Statistics Manual, Dover Publications, Inc., New York, NY, 1960, pp. 147-19]:

$$s_{b_j} = s_{y/123\ k}\sqrt{n e_{ij}}$$
$$\beta_j = b_j \pm \left(t_{a/2,n-k-1}\right) \times s_{b_j}$$

This simple correlation has been tested within the bounds of anticipated conditions. The predictions appear to be reasonable for combinations of input parameters representative of the: Near Field Environment (NFE); SDW; SCW; SAW; SCMW; the unusually harsh, simulated crevice corrosion test

of Asphahani (10 wt. % $FeCl_3$); and the conditions predicted during preliminary tests of the LLNL crevice transport model [J. C. Farmer, R. D. McCright, "Crevice Corrosion and Pitting of High-Level Waste Containers: Integration of Deterministic and Probabilistic Models," Paper No. 160, Annual Meeting of the National Association of Corrosion Engineers (NACE), Corrosion 98, San Diego, CA March 22-27, 1998]. The worst case within the bounds of the regression analysis is the simulated crevice condition used by Asphahani (10 wt. % $FeCl_3$). In the repository, the concentration of $FeCl_3$ is expected to be limited to much lower values by the presence of carbonate, which precipitates iron. **It must be noted that combinations of input parameters that are clearly beyond the range of the data included in the correlation cannot be used to generate reasonable predictions. Therefore, this correlation should not be used for saturated solutions of J-13 and/or $FeCl_3$. With in the limits of the experimental data, predictions are believed to be good representations of the observations.**

For completeness, the above correlation also included observations of passive corrosion rate inferred from Ajit Roy's cyclic polarization measurements. It is well known that the corrosion (or penetration) rate of an alloy, dp/dt, can also be calculated from the corrosion current density, i_{corr}, as follows:

$$\frac{dp}{dt} = \frac{i_{corr}}{\rho_{alloy} n_{alloy} F}$$

where ρ_{alloy} is the density of the alloy, assumed to be approximately 8.4 g cm^{-3}, and F is Faraday's constant. The number of gram equivalents per gram of alloy, n_{alloy}, is calculated with the following equation:

$$n_{alloy} = \sum_j \left(\frac{f_j n_j}{a_j} \right)$$

where f_j is the mass fraction of the j-th alloying element in the material, n_j are the number of electrons involved in the anodic dissolution process, which is assumed to be congruent, and a_j is the atomic weight of the j-th alloying element. These equations have been used to calculate penetration rates for Alloy C-22 from apparent corrosion currents determined during cyclic polarization measurements. In principle, such electrochemically-determined rates should be consistent with those observed in the LTCTF, though experience indicates that such electrochemically-determined rates are conservative (higher than those actually observed).

The magnitude of the observed rates shown in Figure 3 appear to be consistent with those quoted in the article by Smailos, Schwarzkopf, and Koster [E. Smailos, W. Schwarzkopf, R. Koster, "Corrosion Behaviour of Container Materials for the Disposal of High-Level Wastes in Rock Salt Formations," Nuclear Science and Technology, Commission of the European Communities, DUR 10400, 1986], though the correlation cannot be used at such high salt concentration since data from experiments with saturated solutions were not included in the correlation. Penetration rates for Alloy C-4 in a concentrated brine at 90, 170 and 200°C are given. The authors state: "Hastelloy C-4 has also resisted pitting corrosion and stress corrosion cracking, in the absence of irradiation, and its corrosion rate has been low at all testing temperatures (< 1 microns/yr), but it has been attacked by crevice corrosion." The authors go on to state that when it is exposed to gamma irradiation at ~10^5 rad/hr, pitting corrosion was observed. This pitting corrosion is believed by several investigators in the field to be due to the formation of oxidants such as H_2O_2, which shift the corrosion potential in the anodic direction, closer

to the pitting and repassivation potential. At LLNL in the mid 1980's, Glass performed definitive radiolysis experiments showing that the corrosion potential of 316L stainless steel in 0.018 M NaCl at 30°C shifted from approximately –100 mV vs. SCE to approximately +100 mV vs. SCE when exposed to gamma irradiation ($3.3x10^6$ rad/hr) from a Co-60 source [R. S. Glass et al., Gamma Radiation Effects on Corrosion: I. Electrochemical Mechanisms for the Aqueous Corrosion Processes of Austenitic Stainless Steels Relevant to Nuclear Waste Disposal in Tuff, Corrosion Science, Vol. 26, No. 8, 1986, p. 577-590; J. C. Farmer et al., "Corrosion Models for Performance Assessment of High-Level Radioactive-Waste Containers," Nuclear Engineering & Design, Vol. 129, 1991, pp. 57-88]. The level of radiation expected at the outer surface of the CRM at the instant of CAM penetration is estimated to be orders-of-magnitude less than these exposures (10^5-10^6 rad/hr). At the Appendix 7 Meeting held at LLNL in February, 1998, the NRC said that they are ignoring the effects of radiolysis on corrosion, and believe that they are well justified in doing so. Note that radiolysis could form other oxidants, such as chlorine free radicals, ozone, and perhaps even unanticipated species such as peroxydisulfate, which has a very anodic redox potential. However, at low levels of radiation, the effects are not expected to be great. In regard to the C-4 penetration rate data, it must be noted that at high temperature, the expected rates for C-22 would be expected to be lower, as shown in Table 4. In regard to this table, two rates attact particular attention: Alloy C, 5 wt. % $FeCl_3$, 50°C, 0.075 mm crevice; Alloy C-276, H_2SO_4+HCl+$FeCl_3$+ $CuCl_2$, 50°C.

Table 4. Published Penetration Rates (microns/yr) for Various Candidate CRM Alloys.

Exposure	T (°C)	C	C-4	C-276	C-22	Source
10 wt. % $FeCl_3$	25		7.6	5.1	2.5	Haynes, 1987
10 wt. % $FeCl_3$	50		12.7	2.5	2.5	Haynes, 1987
10 wt. % $FeCl_3$	75		**508**	12.7	12.7	Haynes, 1987
5 wt. % $FeCl_3$	50	20				Jackson & van Rooyen, 1972
5 wt. % $CuCl_2$	50	10				Jackson & van Rooyen, 1972
5 wt. % NaOCl	50	6				Jackson & van Rooyen, 1972
5 wt. % $FeCl_3$ + 5 wt. % HCl	25	20				Jackson & van Rooyen, 1972
5 wt. % $FeCl_3$***	50	**5200**				Jackson & van Rooyen, 1972
10 wt. % $FeCl_3$	25			5.08		Asphahani, 1980
10 wt. % $FeCl_3$	50			5.08		Asphahani, 1980
Sea Water, Surface**	25			Nil		Hack, 1983
Sea Water, 2370-6780 ft**				Nil		Reinhart, 1969 (~24 samples)
7 vol. % H_2SO_4 + 3 vol. % HCl + 1 wt. % $FeCl_3$ + 1 wt. % $CuCl_2$	25			7.62		Asphahani, 1980
7 vol. % H_2SO_4 + 3 vol. % HCl + 1 wt. % $FeCl_3$ + 1 wt. % $CuCl_2$	50			**610**		Asphahani, 1980

*Nomenclature: **Crevice sample *** Tight crevice – 0.075 mm*

Such high rates have not been observed with Alloy C-22 samples, configured in tight crevice geometries, and exposed to acidified (pH~2.7), concentrated (1000X) J-13 well water at 90°C. In cases where such high rates have been observed with lesser alloys such as C-4, the observed penetration rates for C-22 have remained low [Haynes, 1987, 10 wt. % $FeCl_3$]. This raises three important questions: (a) can the NRC repassivation potential criterion be applied to Alloys C, C-4 and

C-276 in cases where large penetration rates are predicted; (b) are measured penetration rates for Alloys C, C-4, and C-276 in mixed strong acids really indicative of the rates expected for C-22 in relevant repository environments; (c) are the $FeCl_3$ environments reasonable simulations of a crevice; and (d) is the gradient in electric potential, or electric field, sufficient to induce complete separation of alkali metal cations and halide/oxy anions, thereby producing such an environment.? In regard to the last question, predictions based upon electic double layer theory indicate that electric fields of 10^9 V/cm at the electrode-electrolyte interface (across the compact double layer) may be possible. The field in the diffuse double layer is much less. The extreme field strengths in the compact double layer are believed to be sufficient to induce complete charge separation. However, since such gradients do not exist in the bulk electrolyte found in crevices, pits and cracks, what physical process could be responsible for creating concentrated mixtures of H_2SO_4 and HCl? What plausible scenario can we provide to create environments where such high penetration rats have been observed?

Values for 1000X J-13 are based upon the above correlation, since the chloride concentration is within the range of data included in the correlation [J. C. Farmer et al., "Development of Corrosion Models for High-Level Waste Containers," Proc. 6th International Conference on Nuclear Engineering, ICONE-6, San Diego, CA, May 10-15, 1998, ASME, 1998, 13 p.]. In the case of saturated J-13, estimates are based upon the article by Smailos, Schwarzkopf, and Koster [E. Smailos, W. Schwarzkopf, R. Koster, "Corrosion Behaviour of Container Materials for the Disposal of High-Level Wastes in Rock Salt Formations," Nuclear Science and Technology, Commission of the European Communities, DUR 10400, 1986], as interpreted by another member of the Expert Elicitation Panel [D. Shoesmith, "Passive Corrosion of the CRM," electronic mail message, February 13, 1998]. The data quoted by Shoesmith is for "Q-Brine" and "Z-Brine" electrolytes, as shown Table 5a.

Table 5a. Data for Passive Corrosion of Alloy C-4 in Saturated Brines (Smailos et al.; Shoesmith).

Brine	pH	NaCl	KCl	$MgCl_2$	$MgSO_4$	H_2O	90°C Rate	170°C Rate	pH
		wt. %	wt. %	wt. %	wt. %	wt. %	μm/yr	μm/yr	Shoesmith
Q	4.9	1.4	4.7	26.8	1.4	65.7	0.02	0.15-0.66	~5
Z	3.6	0.2	0.66	36.4	0.87	61.9	10-14		~2

The rate of 10-14 microns/yr for Alloy C-4 in Z-Brine at 90°C is interpreted as the "maximum possible" value by Shoesmith (taken here as rate at 99th percentile). According to page 10 of the Smailos Report: "After three years of exposure until now Hastelloy C-4 has remained resistant to pitting corrosion, and to stress corrosion cracking. At 90°C local crevice corrosion attacks occurred at single points at the metal/PTFE and metal/metal contact surfaces with maxiumum depths of 250 microns (metal/PTFE), and 20-70 microns (metal/metal), respectively." This translates into a maximum penetration rate of 15-51 microns/yr. It must be noted that the rates from the Smailos et al. Report had to be scaled for pH and temperature so that all conditions of interest in this elicitation could be covered. While the base rate used was taken from the "Z-Brine" data, the activation energy used to scale the rate for temperature had to be inferred from the "Q-Brine" data. A very reasonable value of the activation energy, E_a, was estimated to be approximately 12 kcal/mol. The estimate was made with the following equation, which is based upon an Ahrenius-type rate expression:

$$\frac{r_1}{r_2} = \exp\left[\frac{E_a}{R}\left(\frac{1}{T_2} - \frac{1}{T_1}\right)\right]$$

At 170°C (T_1), the observed penetration rates were given as 0.66 amnd 0.15 microns/yr, which were averaged to give a single value of 0.4 microns/yr (r_1). At a lower temperature of 90°C (T_2), the observed rate was given as 0.02 microns/yr (r_2). Rates were scaled with the pH as implied by the correlation, since no better means of estimating the response is available. Therefore, the rates were assumed to obey the following empirical law:

$$\frac{r_1}{r_2} = \exp\left[0.87409\left(pH_2 - pH_1\right)\right]$$

Establishment of CDF's for 1000X and saturated J-13 cases require estimation distribution width about the mean. In regard to estimates based upon either the correlation and Shoesmith's interpretation of data published by Smailos et al., it was assumed that *logarithimic rates* were distributed normally about the *mean logarithmic rate*. To determine the CDF's for 1000X J-13, which was based upon the correlation, the following simplifying approximations were made:

$$y = \ln\left[\frac{\Delta p}{\Delta t}\right]$$

$$y_{5\%} \approx y_{predicted} - \delta\, y_{\alpha=0.05} \approx y_{predicted} - t_{\alpha=0\,05} s_{123\ k}$$

$$y_{95\%} \approx y_{predicted} + \delta\, y_{\alpha=0\,05} \approx y_{predicted} + t_{\alpha=0\,05} s_{y/123\ k}$$

$$t_{\alpha=0.05} \approx 1.70$$

$$y_{1\%} \approx y_{predicted} - \delta\, y_{\alpha=0\,01} \approx y_{predicted} - t_{\alpha=0\,01} s_{y/123\ k}$$

$$y_{99\%} \approx y_{predicted} + \delta\, y_{\alpha=0.01} \approx y_{predicted} + t_{\alpha=0\,01} s_{y/123\ k}$$

$$t_{\alpha=0\,01} \approx 2.46$$

$$r_{5\%} = \left[\frac{\Delta p}{\Delta t}\right]_{5\%} \approx \exp\left[y_{predicted} - 1.70 \times s_{y/123\ k}\right]$$

$$r_{95\%} = \left[\frac{\Delta p}{\Delta t}\right]_{95\%} \approx \exp\left[y_{predicted} + 1.70 \times s_{y/123\ k}\right]$$

$$r_{1\%} = \left[\frac{\Delta p}{\Delta t}\right]_{1\%} \approx \exp\left[y_{predicted} - 2.46 \times s_{y/123\ k}\right]$$

$$r_{99\%} = \left[\frac{\Delta p}{\Delta t}\right]_{99\%} \approx \exp\left[y_{predicted} + 2.46 \times s_{y/123\ k}\right]$$

The CDF's based upon Smailos et al. assumed values at the 99th and 50th percentiles, and then assumed a log-normal distribution to estimate values at other percentiles. In this case, the standard deviation was estimated to be about 1.6228, the value of $u_{\alpha=0.05}$ was assumed to be 1.645 and the value of $u_{\alpha=0.01}$ was assumed to be 2.326. Based on the foregoing considerations, this member of the Expert Elicitation Panel proposes estimates for passive corrosion rates of the CRM represented by the CDF's summarized in Table 5b. Bold-face values correspond to rates taken from Table 5a.

Table 5b. Estimates of CDF's for Passive Corrosion Rates of Alloy C-22 with Dripping.

Data Source		Regression (Farmer)	Regression (Farmer)	Regression (Farmer)	Smailos (Shoesmith)	Smailos (Shoesmith)	Smailos (Shoesmith)	Smailos (Shoesmith)
Environment		1000X J-13	1000X J-13	1000X J-13	Z-Brine	Z-Brine	Z-Brine	Z-Brine
NaCl (wt. %)		1.2	1.2	1.2	Saturated	Saturated	Saturated	Saturated
T (°C)		25	50	100	90	25	50	100
Percentile (%)	pH	microns/yr	microns/yr	microns/yr	microns/yr	microns/yr	microns/yr	microns/yr
50	1	4.36×10^{-3}	1.85×10^{-2}	1.86×10^{-1}	6.60×10^{-1}	1.71×10^{-2}	8.29×10^{-2}	1.03
50	2	1.82×10^{-3}	7.71×10^{-3}	7.74×10^{-2}	2.75×10^{-1}	7.13×10^{-3}	3.46×10^{-2}	4.31×10^{-1}
50	3	7.59×10^{-4}	3.22×10^{-3}	3.23×10^{-2}	1.15×10^{-1}	2.98×10^{-3}	1.44×10^{-2}	1.80×10^{-1}
50	5	1.32×10^{-4}	5.60×10^{-4}	5.62×10^{-3}	**2.00×10^{-2}**	5.18×10^{-4}	2.51×10^{-3}	3.13×10^{-2}
50	7	2.30×10^{-5}	9.75×10^{-5}	9.79×10^{-4}	3.48×10^{-3}	9.02×10^{-5}	4.38×10^{-4}	5.46×10^{-3}
50	10	1.67×10^{-6}	7.08×10^{-6}	7.11×10^{-5}	2.53×10^{-4}	6.55×10^{-6}	3.18×10^{-5}	3.96×10^{-4}
Percentile (%)	pH	microns/yr	microns/yr	microns/yr	microns/yr	microns/yr	microns/yr	microns/yr
5	1	3.35×10^{-4}	1.42×10^{-3}	1.43×10^{-2}	4.57×10^{-2}	1.18×10^{-3}	5.75×10^{-3}	7.16×10^{-2}
5	2	1.40×10^{-4}	5.93×10^{-4}	5.95×10^{-3}	1.91×10^{-2}	4.94×10^{-4}	2.40×10^{-3}	2.99×10^{-2}
5	3	5.84×10^{-5}	2.47×10^{-4}	2.48×10^{-3}	7.96×10^{-3}	2.06×10^{-4}	1.00×10^{-3}	1.25×10^{-2}
5	5	1.02×10^{-5}	4.31×10^{-5}	4.32×10^{-4}	1.39×10^{-3}	3.59×10^{-5}	1.74×10^{-4}	2.17×10^{-3}
5	7	1.77×10^{-6}	7.49×10^{-6}	7.53×10^{-5}	2.41×10^{-4}	6.25×10^{-6}	3.03×10^{-5}	3.78×10^{-4}
5	10	1.29×10^{-7}	5.44×10^{-7}	5.47×10^{-6}	1.75×10^{-5}	4.54×10^{-7}	2.20×10^{-6}	2.75×10^{-5}
Percentile (%)	pH	microns/yr	microns/yr	microns/yr	microns/yr	microns/yr	microns/yr	microns/yr
95	1	5.67×10^{-2}	2.40×10^{-1}	2.41	9.52	2.47×10^{-1}	1.20	14.9
95	2	2.37×10^{-2}	1.00×10^{-1}	1.01	3.97	1.03×10^{-1}	4.99×10^{-1}	6.23
95	3	9.88×10^{-3}	4.19×10^{-2}	4.20×10^{-1}	1.66	4.30×10^{-2}	2.08×10^{-1}	2.60
95	5	1.72×10^{-3}	7.29×10^{-3}	7.32×10^{-2}	2.89×10^{-1}	7.48×10^{-3}	3.63×10^{-2}	4.52×10^{-1}
95	7	2.99×10^{-4}	1.27×10^{-3}	1.27×10^{-2}	5.03×10^{-2}	1.30×10^{-3}	6.31×10^{-3}	7.87×10^{-2}
95	10	2.17×10^{-5}	9.21×10^{-5}	9.25×10^{-4}	3.65×10^{-3}	9.46×10^{-5}	4.59×10^{-4}	5.72×10^{-3}
Percentile (%)	pH	microns/yr	microns/yr	microns/yr	microns/yr	microns/yr	microns/yr	microns/yr
1	1	1.06×10^{-4}	4.51×10^{-4}	4.53×10^{-3}	1.51×10^{-2}	3.92×10^{-4}	1.90×10^{-3}	2.37×10^{-2}
1	2	4.44×10^{-5}	1.88×10^{-4}	1.89×10^{-3}	6.32×10^{-3}	1.64×10^{-4}	7.94×10^{-4}	9.90×10^{-3}
1	3	1.85×10^{-5}	7.85×10^{-5}	7.89×10^{-4}	2.64×10^{-3}	6.83×10^{-5}	3.31×10^{-4}	4.13×10^{-3}
1	5	3.23×10^{-6}	1.37×10^{-5}	1.37×10^{-4}	4.59×10^{-4}	1.19×10^{-5}	5.77×10^{-5}	7.19×10^{-4}
1	7	5.62×10^{-7}	2.38×10^{-6}	2.39×10^{-5}	7.99×10^{-5}	2.07×10^{-6}	1.00×10^{-5}	1.25×10^{-4}
1	10	4.08×10^{-8}	1.73×10^{-7}	1.74×10^{-6}	5.80×10^{-6}	1.50×10^{-7}	7.29×10^{-7}	9.09×10^{-6}
Percentile (%)	pH	microns/yr	microns/yr	microns/yr	microns/yr	microns/yr	microns/yr	microns/yr
99	1	1.79×10^{-1}	7.57×10^{-1}	7.60	28.8	7.45×10^{-1}	3.61	45.1
99	2	7.45×10^{-2}	3.16×10^{-1}	3.17	**12.0**	3.11×10^{-1}	1.51	18.8
99	3	3.11×10^{-2}	1.32×10^{-1}	1.32	5.01	1.30×10^{-1}	6.29×10^{-1}	7.84
99	5	5.41×10^{-3}	2.29×10^{-2}	2.30×10^{-1}	8.72×10^{-1}	2.26×10^{-2}	1.10×10^{-1}	1.37
99	7	9.43×10^{-4}	3.99×10^{-3}	4.01×10^{-2}	1.52×10^{-1}	3.93×10^{-3}	1.91×10^{-2}	2.38×10^{-1}
99	10	6.85×10^{-5}	2.90×10^{-4}	2.91×10^{-3}	1.10×10^{-2}	2.86×10^{-4}	1.39×10^{-3}	1.73×10^{-2}

Estimates for humid air corrosion assume rates comparable to those for aqueous-phase passive corrosion at neutral pH, which appears to be more or less consistent with the impressive "mirror finish" of an Alloy C sample after 56 years exposure to a coastal environment on the coast of North Carolina (Table 5c).

Table 5c. Estimates of CDF's for Passive Corrosion Rates of Alloy C-22 in Humid Air – Humid Air Corrosion.

T (°C)	25	50	100
Percentile (%)	microns/yr	microns/yr	microns/yr
1	5.62×10^{-7}	2.38×10^{-6}	2.39×10^{-5}
5	1.77×10^{-6}	7.49×10^{-6}	7.53×10^{-5}
50	2.30×10^{-5}	9.75×10^{-5}	9.79×10^{-4}
95	2.99×10^{-4}	1.27×10^{-3}	1.27×10^{-2}
99	9.43×10^{-4}	3.99×10^{-3}	4.01×10^{-2}

PIT INITIATION PROBABILITY

Questions:

3) What is the probability of initiating localized (crevice) corrosion of the inner barrier under the following conditions?

T = 25°C
1) pH 2.5 and potential of 340 mV and 640 mV vs. SHE
2) pH 3-10 and potential of 340 mV vs. SHE

T = 50°C
1) pH 2.5 and potential of 340 mV and 640 mV vs. SHE
2) pH 3-10 and potential of 340 mV vs. SHE

T = 100°C
1) pH 2.5 and potential of 340 mV and 640 mV vs. SHE
2) pH 3-10 and potential of 340 mV vs. SHE

Response:

The probability of localized corrosion, which is assumed to include both crevice corrosion and pit initiation, is based upon observations of the pitting and repassivation potential. First, all observed values are placed on a common potential scale, that of the standard hydrogen electrode (SHE). Correlations have been obtained for the electrochemical potentials of the AgCl and SCE reference electrodes as functions of temperature. The first correlation for Ag/AgCl/0.1M KCl was provided by David Shoesmith and was developed by AECL [King et al., "A High-Temperature, High-Pressure, Silver-Silver Chloride Reference Electrode: A User's Guide," AECL-9890, 1989].

$$E_{AgCl}(SHE) = 0.23755 - 5.3783\times10^{-4}T(°C) - 2.3728\times10^{-6}T(°C)^2 + 2.2671\times10^{-4}[T(°C)+273]$$

The second correlation for Hg/Hg_2Cl_2/satd. KCl was obtained from the well-known text by Bard & Faulkner [A. J. Bard, L. R. Faulkner, Electrochemical Methods, Fundamentals and Applications, John Wiley & Sons, New York, NY, 1980].

$$E_{SCE}(SHE) = 0.2412 - 6.61\times10^{-4}[T(°C) - 25] - 1.75\times10^{-6}[T(°C) - 25]^2 - 9.0\times10^{-10}[T(°C) - 25]^3$$

Relevant temperature corrections can be calculated with each of these expressions, as given in Table 6 below:

Table 6. Correction of Reference Electrodes for Excursions from Ambient Temperature.

T (°C)	$E_{Ag/AgCl/0\ 1M\ KCl}$ (V vs. SHE)	E_{SCE} (V vs. SHE)
25	0.2902	0.2412
60	0.2722	0.2344
90	0.2629	0.1906
95	0.2485	0.1861

In the case of the Ag/AgCl/0.1M KCl electrode, the potential must also be corrected for electrolyte concentration, so that it is applicable for the standard AgCl electrode with saturated KCl. First, the solubility of KCl as a function of temperature is obtained from the CRC Handbook [CRC Handbook, Chemical Rubber Company, 61st Edition, 1980-81, p. B-132].

$$T = 20°C: \quad C_{saturated\ KCl} = 23.8\ grams\ per\ 100\ cc$$

$$T = 100°C: \quad C_{saturated\ KCl} = 56.7\ grams\ per\ 100\ cc$$

The saturation concentrations at other temperatures is estimated by simple linear interpolation, as shown in Table 7:

Table 7. Saturation Concentration of KCl by Linear Interpolation.

T (°C)	$C_{saturated\ KCl}$ (g per100 cc)	$C_{saturated\ KCl}$ (mol/kg)
20	23.8	3.192
25	25.86	3.468
60	40.25	5.398
90	52.59	7.053
95	54.64	7.329
100	56.7	7.605

Note that a formula weight of KCl is assumed to be approximately 74.56, and ignores any hydration effects. Obviously, we have ignored activity coefficients. The Debye-Huckel equation could be used to esitmate the activity coefficients, however, it only applies rigorously to infinitely dilute solutions. Other activity coefficient models for higher electrolyte concentrations are controversial, due to a general lack of knowledge of the sphere of hydration surrounding individual ions, a general inability to account for Coulombic and dipole interactions between each pair of individual ions, and other equally important effects. A simplification of the Nernst equation, which also ignores activity coefficients, can be used to make a first order correction of the potential of the Ag/AgCl/KCl reference electrode for KCl concentration. The Nernst equation can be written as:

$$E = E^0 + \frac{RT}{nF}\ln\frac{C_O}{C_R}$$

where the convention is assumed to be:

$$O + ne^- \xrightarrow{electrode} R$$

Application of this simplified Nernst equation to the Ag/AgCl/KCl reference electrode yields:

$$E_{Ag/AgCl/satd\ KCl} - E_{Ag/AgCl/0.1M\ KCl} = -\frac{RT}{F}\ln\frac{C_{satd.KCl}}{C_{0.1M\ KCl}}$$

where the assumed reaction is:

$$AgCl + e^- \longrightarrow Ag + Cl^-$$

Given Faraday's constant of 9.64846×10^4 C/equiv, the value of RT/F at 25°C is 0.02569 V, and can be scaled to different temperatures (Table 8). Application of these corrections to measured corrosion, pitting, and repassivation potentials is summarized in Tables 9a and 9b. Note that the interpretation of cyclic polarization (CP) curves is very subjective. Where more than one inflection point might be interpreted as the potential of interest, the most conservative value was chosen (least anodic repassivation potential, for example). These data are summarized in Figure 4.

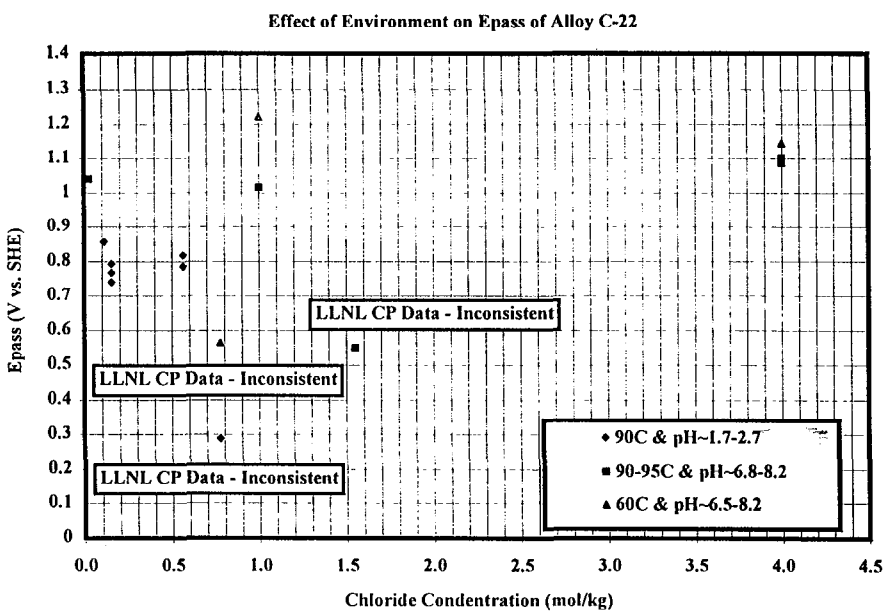

Figure 4. Observations of repassivation potential as a function of chloride, temperature, and pH.

Table 8. Correction of Ag/AgCl Reference Electrode Potenial for Concentration.

T (°C)	RT/F (V)	$E_{Ag/AgCl/0.1M\ KCl}$ (V vs. SHE)	$C_{saturated\ KCl}$ (mol/kg)	Concentration Correction (V)	$E_{Ag/AgCl/satd\ KCl}$ (V vs. SHE)	E_{SCE} (V vs. SHE)
25	0.02569	0.2902	3.468	-0.0911	0.1991	0.2412
60	0.02871	0.2722	5.398	-0.1145	0.1577	0.2344
90	0.03129	0.2629	7.053	-0.1332	0.1297	0.1906
95	0.03172	0.2485	7.329	-0.1362	0.1123	0.1861

Table 9a. Corrosion and Threshold Potentials (vs. SHE) for Alloy C-22 Measured by LLNL & NRC.

Source	ID	T	T	NaCl	$FeCl_3$	Cl^-	pH	E_{corr}	E_{pit} - low	E_{pit} - high	E_{pass}
		C	K	Wt. %	Wt. %	mol/kg		V vs. Ref.	V vs. Ref.	V vs. Ref.	V vs. Ref.
LLNL	090996C1	90	363	10.00	0	1.552	6.83	-0.154	0.312	0.312	0.42
LLNL	103397C1	90	363	1.00	0	0.155	2.69	-0.159	0.628	0.733	0.663
LLNL	102497C2	90	363	1.00	0	0.155	2.67	-0.162	0.628	0.785	0.611
LLNL	102797C1	90	363	5.00	0	0.776	2.69	-0.202	0.423	0.654	0.158
LLNL	081997C1	90	363	1.00	0	0.155	2.69	-0.145	0.59	0.687	0.638
LLNL	082697C2	60	333	5.00	0	0.776	6.53	-0.105	0.393	0.448	0.407
LLNL	110497C2	90	363	0.00	0.61	0.113	2.14	0.531	0.775	0.829	0.727
LLNL	103097C1	90	363	0.00	3.05	0.564	1.72	0.584	0.759	0.766	0.655
LLNL	103197C2	90	363	0.00	3.05	0.564	1.72	0.439	0.838	0.872	0.688
NRC	C22-1	95	368	25.78	0	4.000	8.2				0.916
NRC	C22-2	95	368	25.78	0	4.000	8.2				0.911
NRC	C22-3	95	368	25.78	0	4.000	8.2				0.9
NRC	C22-4	60	333	25.78	0	4.000	8.2				0.911
NRC	C22-5	95	368	6.44	0	1.000	8.2				0.829
NRC	C22-6	60	333	6.44	0	1.000	8.2				0.986
NRC	C22-7	95	368	0.18	0	0.028	8.2				0.854

Table 9b. Corrosion and Threshold Potentials (vs. SHE) for Alloy C-22 Measured by LLNL & NRC.

ID	Reference	Correction	Ecorr	Epit - low	Epit - high	Epass	Comments
		V	V vs. SHE	V vs. SHE	V vs. SHE	V vs. SHE	
090996C1	Ag/AgCl/KCl	0.1297	-0.0243	0.4417	0.4417	0.5497	inconsistent
103397C1	Ag/AgCl/KCl	0.1297	-0.0293	0.7577	0.8627	0.7927	
102497C2	Ag/AgCl/KCl	0.1297	-0.0323	0.7577	0.9147	0.7407	
102797C1	Ag/AgCl/KCl	0.1297	-0.0723	0.5527	0.7837	0.2877	inconsistent
081997C1	Ag/AgCl/KCl	0.1297	-0.0153	0.7197	0.8167	0.7677	
082697C2	Ag/AgCl/KCl	0.1577	0.0527	0.5507	0.6057	0.5647	inconsistent
110497C2	Ag/AgCl/KCl	0.1297	0.6607	0.9047	0.9587	0.8567	
103097C1	Ag/AgCl/KCl	0.1297	0.7137	0.8887	0.8957	0.7847	
103197C2	Ag/AgCl/KCl	0.1297	0.5687	0.9677	1.0017	0.8177	
C22-1	SCE	0.1861				1.1021	
C22-2	SCE	0.1861				1.0971	
C22-3	SCE	0.1861				1.0861	
C22-4	SCE	0.2344				1.1454	
C22-5	SCE	0.1861				1.0151	
C22-6	SCE	0.2344				1.2204	
C22-7	SCE	0.1861				1.0401	

The probability of initiating localized corrosion are based on the stochastic probability theory of pit initiation, as discussed by Baroux [B. Baroux, "Further Insights on the Pitting Corrosion of Stainless Steels," Chapter 9, Corrosion Mechanisms in Theory and Practice, P. Marcus, J. Oudar, Eds., Marcel Dekker, Inc., New York, NY, pp. 265-309]. First, the expression for the survival probability is:

$$\delta P_S = 1 - \overline{\omega} \times \delta S$$

where δP is the survival probability (probability of no pitting) of an infinitesimal area δS on a sample of area S. The survival probability of the entire surface S is then:

$$P_S = \left[1 - \bar{\omega} \times \delta S\right]^{\frac{S}{\delta S}}$$

The pit generation rate, PGR, is then defined in terms of the time derivative of the elementary pitting probability:

$$\frac{d\bar{\omega}}{dt} = g = PGR$$

$$\bar{\omega} = \int_0^t (PGR)dt$$

We then make the following simplification by assuming that PGR is independent of time and that δS ~ S. While it would be better to avoid such gross over simplification, it does provide some degree of insight into the expected dependence of the survival probability, and the probability of pit initiation, on electrochemical potential. This insight is needed to address the question regarding probability of pitting.

$$P_S \approx 1 - PGR \times t \times S$$

The probability of pitting (localized corrosion, LC) is then assumed to be:

$$P_{LC} \approx PGR \times t \times S$$

It is observed empirically that:

$$\ln(PGR) \approx \beta (E - E_{pit})$$

Therefore:

$$\ln\left(\frac{P_{LC,1}}{P_{LC,2}}\right) \approx \ln\left(\frac{PGR_1}{PGR_2}\right) \approx \beta (E_1 - E_2)$$

We can estimate the empirical constant β as:

$$\beta = \frac{\ln(P_{LC,1}/P_{LC,2})}{(E_1 - E_2)}$$

Now, for illustration, consider a hypothetical case where the repassivation potential is assumed to be the point at which there is a 5% chance of initiating localized corrosion. Furthermore, assume that the average repassivation potential is 800 mV vs. SHE, and that the observed scatter around the averate ± 50 mV. The probability of initiating localized corrosion at 800 mV vs. SHE is assumed to be 5%, and

the probability of initiating localized corrosion at 800-50 mV vs. SHE is assumed to be 1%. In this case,

$$\beta = \frac{\ln(5/1)}{(800\,mV - 750\,mV)} \approx 0.032\,mV^{-1}$$

The CDF based upon these simplification and assumptions are summarized in Table 10a, where the recommended case is Case 3. It should be noted that the maximum probability of pitting is believed to be less than a 15% (99th percentile, pH 2.5, 640 mV), with typical values of 0.01-2.12% (Table 10b).

4) What is the localized corrosion rate of the C-22 inner barrier?

The expert assessments to date have provided two alternative ways to model localized corrosion of the inner barrier: a) "exponential" pit growth law, and b) "logarithmic" pit growth law: Exponential crevice growth law is expressed as follows:

$$p = B \times t^{n}$$

where p is the crevice depth, B is a constant, t is time, and n is an exponent. Distributions for the constants B and n have been provided. A crevice corrosion model suggested recently by LLNL belongs to this type (n = ½ corresponding to a diffusion-controlled penetration rate). Logarithmic crevice growth law is expressed as follows:

$$p = k \times \exp\left[\frac{Q}{T}\right] \times \log[t] - x_0$$

where k, Q and x_0 are constants, T is temperature, and t is time. Distributions for the constants k, Q and x_0 have been provided. Please express your assessment of corrosion rate using either of these functional forms (or another of your choice). Please consider the following conditions:

T = 25°C
1) pH 2.5 and potential of 340 mV and 640 mV vs. SHE
2) pH 3-10 and potential of 340 mV vs. SHE

T = 50°C
1) pH 2.5 and potential of 340 mV and 640 mV vs. SHE
2) pH 3-10 and potential of 340 mV vs. SHE

T = 100°C
1) pH 2.5 and potential of 340 mV and 640 mV vs. SHE
2) pH 3-10 and potential of 340 mV vs. SHE

Uncertainties in the coefficients of the growth laws should be expressed by, as a minimum, the 0th and 100th percentile values along with the median, 5th percentile and 95th percentile values.

Response:

As pointed out by Prof. Scully, the "logarithmic" expression has some very attractive features. However, there is an obvious inconsistency in the expression as presented in the elicitation question. It

is recommended that this be resolved by using log(1+t) instead of log(t). This Panel member prefers the "exponential form" since it is easily interpreted in terms of diffusion-controlled penetration or other easily visualized phenomena. The penetration rates for localized corrosion shown in Tables 12 are based on Asphahani's data for Alloys C-22 and C-276, which are summarized in Tables 4 and 11, respectively. These data can also be found in Tables 22 and 23 of Gdowski's degradation mode survey, respectively [G. E. Gdowski, "Survey of Degradation Modes of Four Nickel-Chromium-Molybdenum Alloys," UCRL-ID-108330, March, 1991, pp. 30-31]. Specific points used to generate Table 12 are in bold-face type. In the case of localized corrosion at 340 mV vs. SHE, it is assumed that the penetration rates are similar to those observed for Alloy C-22 in simulated crevice solutions (accelerated passive corrosion in 10 wt. % $FeCl_3$). In the case of localized corrosion at 640 mV vs. SHE, it is assumed that the penetration rates are similar to those observed for Alloy 625 (active crevice in 10 wt. % $FeCl_3$ and and active pitting corrosion in "green death" solution). The apparent activation energy is assumed to be 20 kcal/mol, which is close to that observed for many chemical reactions. Note the rapid wall penetration at high applied potential (640 mV vs. NHE) and low pH (2.5).

Table 10a. Probabilities of Localized Corrosion Initiation on Alloy C-22 – Estimated CDF's.

Case 1: P = 5% at E_{pass} & P = 1% at $E_{pass,low}$	**Environment A**	**Environment B**	**Environment C**
PH	2.5	2.5	5 to 7
E (mV vs. SHE)	340	640	340
β at 25°C	8.05×10^{-3}	8.05×10^{-3}	8.05×10^{-3}
β at 50°C	8.05×10^{-3}	8.05×10^{-3}	8.05×10^{-3}
β at 100°C	8.05×10^{-3}	8.05×10^{-3}	8.05×10^{-3}
P at 25°C	0.0368	0.4123	0.0074
P at 50°C	0.0824	0.9221	0.0165
P at 100°C	0.1843	2.0625	0.0368
Case 2: P = 50% at E_{pass} & P = 5% at $E_{pass,low}$	**Environment A**	**Environment B**	**Environment C**
pH	2.5	2.5	5 to 7
E (mV vs. SHE)	340	640	340
β at 25°C	1.15×10^{-2}	1.15×10^{-2}	1.15×10^{-2}
β at 50°C	1.15×10^{-2}	1.15×10^{-2}	1.15×10^{-2}
β at 100°C	1.15×10^{-2}	1.15×10^{-2}	1.15×10^{-2}
P at 25°C	0.0449	1.4148	0.0045
P at 50°C	0.1419	4.4684	0.0142
P at 100°C	0.4480	14.1120	0.0449
Case 3: P = 50% at E_{pass} & P = 1% at $E_{pass,low}$	**Environment A**	**Environment B**	**Environment C**
pH	2.5	2.5	5 to 7
E (mV vs. SHE)	340	640	340
β at 25°C	7.82×10^{-3}	7.82×10^{-3}	7.82×10^{-3}
β at 50°C	7.82×10^{-3}	7.82×10^{-3}	7.82×10^{-3}
β at 100°C	7.82×10^{-3}	7.82×10^{-3}	7.82×10^{-3}
P at 25°C	0.0424	0.4427	0.0089
P at 50°C	0.0927	0.9678	0.0194
P at 100°C	0.2026	2.1154	0.0424

Table 10b. Estimated CDF Probabilities (%) for Initiation of Localized Corrosion on Alloy C-22 During Dripping – Based on Table 10a (above) – Aqueous phase (dripping) required for initiation.

Percentile (%)	A/25°C	A/50°C	A/100°C	B/25°C	B/50°C	B/100°C	C/25°C	C/50°C	C/100°C
1	0.0368	0.0824	0.1843	0.4123	0.9221	2.0625	0.0045	0.0142	0.0368
50	0.0424	0.0927	0.2026	0.4427	0.9678	2.1154	0.0074	0.0165	0.0424
99	0.0449	0.1419	0.4480	1.4148	4.4684	14.1120	0.0089	0.0194	0.0449

Table 11. Penetration Rates for Active Localized Corrosion of Alloy 625 (no W) – Not Applicable for Alloy C-22 (contains W) – Observations Provided for Illustration and Contrast.

Crevice Corrosion	Crevice Corrosion	Pitting Corrosion	Pitting Corrosion
25°C	50°C	25°C	102°C
10 wt. % $FeCl_3$	10 wt. % $FeCl_3$	7 vol. % H_2SO_4 + 3 vol. % HCl + 1 wt. % $FeCl_3$ + 1 wt. % $CuCl_2$	7 vol. % H_2SO_4 + 3 vol. % HCl + 1 wt. % $FeCl_3$ + 1 wt. % $CuCl_2$
38.1 microns/yr	3,150 microns/yr	7.62 microns/yr	48,060 microns/yr

Table 12. Penetration Rates for Active Localized Corrosion of Alloy 625 (no W) – Not Applicable for Alloy C-22 (contains W) – CDF's for Parameters in Rate Expression.

pH=2.5							
E=340 mV							
Percentile	n	k (for n=1)	Ea	Q	Depth (1 yr; 25°C; n=1)	Depth (1 yr; 75°C; n=1)	Depth (1000 yr; 60°C; n=1)
%	none	microns/yr	cal/mol	K	microns	microns	cm
0	0	$5.07x10^{12}$	5000	2500	0.01	1.7	0.0461
1	0.1	$7.99x10^{12}$	10000	5000	0.02	2.6	0.0726
5	0.3	$1.26x10^{13}$	15000	7500	0.03	4.2	0.1148
50	0.5	**$3.83x10^{13}$**	20000	10000	0.10	**12.7**	0.3481
95	0.7	$1.16x10^{14}$	25000	12500	0.31	38.5	1.0550
99	0.9	**$9.37x10^{14}$**	30000	15000	**2.50**	310.4	8.5056
100	1	$7.08x10^{15}$	35000	17500	18.89	2345.1	64.2713

pH=2.5							
E=640 mV							
Percentile	n	k (for n=1)	Ea	Q	Depth (1 yr; 50°C; n=1)	Depth (1 yr; 102°C; n=1)	Depth (1000 yr; 60°C; n=1)
%	none	microns/yr	cal/mol	K	microns	microns	cm
0	0	$2.42x10^{15}$	5000	2500	87	6360	22
1	0.1	$3.82x10^{15}$	10000	5000	137	10018	35
5	0.3	$6.04x10^{15}$	15000	7500	217	15855	55
50	0.5	**$1.83x10^{16}$**	**20000**	**10000**	657	**48060**	166
95	0.7	$5.55x10^{16}$	25000	12500	1990	145677	504
99	0.9	**$8.79x10^{16}$**	30000	15000	**3150**	230555	798
100	**1**	$6.64x10^{17}$	35000	17500	23803	1742155	6031

pH=3-10							
E=340 mV							
Percentile	n	k (for n=1)	Ea	Q	Depth (1 yr; 25°C; n=1)	Depth (1 yr; 75°C; n=1)	Depth (1000 yr; 60°C; n=1)
%	none	microns/yr	cal/mol	K	microns	microns	cm
0	0	5.07×10^{12}	5000	2500	0.01	1.7	0.0461
1	0.1	7.99×10^{12}	10000	5000	0.02	2.6	0.0726
5	0.3	1.26×10^{13}	15000	7500	0.03	4.2	0.1148
50	0.5	**3.83×10^{13}**	20000	10000	0.10	**12.7**	0.3481
95	0.7	1.16×10^{14}	25000	12500	0.31	38.5	1.0550
99	0.9	**9.37×10^{14}**	30000	15000	**2.50**	310.4	8.5056
100	1	7.08×10^{15}	35000	17500	18.89	2345.1	64.2713

In regard to pit penetration rates, it must be noted that the current elicitation does not deal with the issue of "stiffling" which leads to the death or a propagating pit. This very important effect has been given emphasis Prof. Scully's presentations and discussion [J. R. Scully, "Appendix D, Elicitation Interview Summaries," Waste Package Degradation Expert Elicitation Project Final Report, K. J. Coppersmith, R. C. Perman, M. Pendleton, J. L. Younker, Civilian Radioactive Waste Management System Management and Operating Contractor, Geomatrix Consultants, San Francisco, CA, August 15, 1997, pp. JS 1-30]. In principle, a pit will cease to grow (die) if the depth becomes so great that the current density at the base of the pit falls below the passive current density. The importance of "stifling" has also been pointed out by Marsh [G. P. Marsh, K. J. Taylor, Z Sooi, "The Kinetics of Pitting Corrosion of Carbon Steel," SKB Technical Report 88-09, Swedish Nuclear Fuel and Waste Management Company (SKB), Box 5864, S-102 48, Stockholm, 1988, 39 p.]. In the case of pit propagation in carbon steel, Marsh gives the following criterion based upon the passive current density, i_{pass}:

$$\frac{i_{pass}}{4F} \le D \left. \frac{\partial C(x,t)}{\partial x} \right|_{x=0}$$

where i_{pass} is the passive current density, F is Faraday's constant, D is the diffusivity, C is concentration, x is the distance into the pit from the mouth of the pit, and t is time. It was noted that careful measurements of i_{pass} are required for any theoretical analysis. The critical concentration gradient across the pit is estimated to be:

$$\left. \frac{\Delta C}{\Delta x} \right|_{critical} \ge \frac{i_{pass}}{4FD}$$

In the case of a multicomponent alloy such as Alloy C-22, the criterion can be expressed in terms of the i-th diffusing species:

$$\left. \frac{\Delta C_i}{\Delta x} \right|_{critical} \ge \frac{f_i}{n_i} \frac{i_{pass}}{FD}$$

where f_i is the mole fraction of the passive current producing the i-th diffusing species, n_i is the the number of electrons involved in the anodic dissolution. If one assumes (a) $f_i = 0.01$, (b) $i_{pass} = 4 \times 10^{-6}$

A/cm^2, (c) $n_i = 6$, (d) $F = 9.64846 \times 10^4$ C/equiv, (e) $D \sim 10^{-5}$ cm^2/sec and (f) $\Delta x = 2$ cm, the critical differential concentration, ΔC_i, is estimated to be 1.38×10^{-8} mol/g (1.38×10^{-5} mol/kg). Note that the solubility of WO_3 is only $\sim 10^{-10}$ mol/kg at pH ~ 2. If any dissolved species at the base of the pit has a solubility less than this limiting value, the pit will die before wall penetration is achieved. Alternatively, given a maximum possible differential concentration, the maximum possible pit depth at stifling (death) can be calculated.

$$\Delta x \leq \frac{n_i F D \Delta C_i}{f_i i_{pass}}$$

The largest differential concentration and the largest critical pit depth occur when the solution at the base of the pit is saturated and when the concentration at the mouth of the pit is zero.

$$\Delta x \leq \frac{n_i F D C_{sat}}{f_i i_{pass}}$$

The solubilities of various oxides and hydroxides believed to be formed during dissolution of Alloy C-22 are given by Pourbaix and are shown in Table 13 [M. Pourbaix, Atlas of Electrochemical Equilibria in Aqueous Solutions, English Translation by J. A. Franklin, Pergamon Press, New York, NY; Cebelcor, Brussels, Belgium, 1966, 644 p]. From the solubility vs. pH curves given by Pourbaix, it appears that the following empirical relationship is obeyed over limited ranges of pH:

$$\log[C_{sat}] = m \times [pH] + b$$

Where C_{sat} is the concentration at saturation, m is the slope and b is the intercept. Values of the slope and intercept were estimated from the curves of Pourbaix and are also given in Table 13. This abstracted model for solubility was used to estimate the logarithims of solubilities given in Table 14, and the solubilities (mol/kg) given in Table 15.

Based upon the estimated solubilites given in Table 15, the critical pit depths were calculated and are given in Tables 16 and 17. Ranges of pH where localized corrosion is stifled by a particular film-forming compound are in bold face type. The pit depth is limited to a different extent by each oxide or hydroxide. At low pH, MoO_3 and WO_3 appear to be primarily responsible for the superior corrosion performance of Alloy C-22. Based upon this calculation, one would expect the localized corrosion of Alloy C-22 to be stifled over the entire range of pH, extending from –1 to 10. This is consistent with observations in acidic media of interest (simulated crevice solution of 10 wt. % $FeCl_3$). There are unusual acidic environments where corrosion is known to occur. Both experience and calculation appear to indicate that pits should not propagate in Alloy C-22 during exposure to crevice conditions.

Clearly, the rates for penetration of the CRM must reflect the stifling of localized attack by Mo- and W-based compounds. This is consistent with a consensus reached by the majority of the Expert Elicitation Panel members during a conference call at noon on Friday, February 27, 1998. Published experimental data obtained with simulated crevice solutions (10 wt. % $FeCl_3$ at 25, 50 and 75°C) and experimental data from tests with crevice samples exposed to simulated acidified J-13 water (SAW) for 1 year (long term tests at LLNL) both indicate penetration by passive corrosion through a protective film. Observed penetration rates of Alloy C-22 show that the corrosion of Alloy C-22 in anticipated crevice solutions is due to passive dissolution, not catastrophic breakdown of the passive

film. In the opinion of this member of the Expert Elicitation Panel, it is therefore appropriate to use the previously discussed correlation of experimental data to estimate penetration rates in the crevice. Such rates are believed to account for the stifling effect of Mo_3 and WO_3. Uncertainties should be treated in the same manner as in the case of passive corrosion rates. This is believed to be more or less consistent with the insight of other members of the Expert Elicitation Panel. Kevin Coppersmith of Geomatrix posed the following question: "What is the rate of localized corrosion on the Alloy C-22 inner barrier once it initiates." Dr. Andresen replied [February 28, 1998]: "The approach adopted by Joe Farmer, e.g., as expressed in his elicitation (earlier version), appear entirely adequate based on our current state of knowledge. Caution must be exercised in determining how long to continue to use a given corrosion rate because, as the waste backage cools even slightly, there is a very strong liklihood that localized corrosion will cease. Because the critical temperature for crevice corrosion is very high for C-22, the probability of initiating (and sustaining) localized corrosion is much lower even at 90°C than 100°C." Please note that we distinguish between "stifled passive corrosion in a crevice" and "classical active crevice corrosion." Dr. Shoesmith replied [March 2, 1998]: "The rate should be scaled according to the B values (and their uncertainties) used by Farmer. A similar activation energy term to that used by Farmer (should be) included. This is Localized Corrosion Model III as presented by Lee in Washington." Boths Drs. Andresen and Shoesmith are internationally renowned for their unusualy high level of expertise in the field of corrosion of nuclear systems. This member believes that such opinions should be heavily weighted. The correlation presented to Drs. Andresen and Shoesmith has been used as the basis of generating the penetration rates for the localized corrosion of Alloy C-22 in Table 18, which are believed to reflect stifling (as per guidance of February 27, 1998). In the case of 1000X J-13, it is assumed that the localized environment can be represented by the following inputs to the correlation, which are within (or close to) the bounds of the correlated data: NaCl = 1.2 wt. %; $FeCl_3$ = 1 wt. %; pH = 1.92. In the case of saturated J-13, is is assumed that the localized environment can be represented by the following inputs to the correlation, which are within (or close to) the bounds of the correlated data: NaCl = 1.2 wt. %; $FeCl_3$ = 10 wt. %; pH = 0.7. In both cases, the NaCl concentration is based upon the "equivalent NaCl concentration" in 1000X J-13. At 1000X J-13 (1.2 wt. % NaCl), the effect of crevice corrosion is accounted for by the assumed presence of 1 wt. % FeCl3 (comparable to NaCl concentration), which would lower the pH to about 1.92 at 25°C (see Table 2). Under saturated conditions, it is assumed that much higher concentrations of chloride will exist at the mouth of the crevice, enabling the $FeCl_3$ inside the crevice to increase to 10 wt. %, which is comparable to the simulated crevice solution used for accelerated testing by Asphahani (see Table 4, Haynes, 1987). From the data given in Table 2, it is believed that the pH of an aqueous solution with 10 wt. % $FeCl_3$ is approximately 0.7.

In regard to the estimated rates given in Table 18, it is assumed that the same penetration rate will be experienced at both 340 and 640 mV vs. SHE. This is comparable to assuming that the passive current density is independent of potential from 340 to 640 mV vs. SHE, which is observed experimentally during some cyclic polarization measurments [quality data of Dr. Ajit Roy, August 28, 1998, 5 wt. % NaCl, pH 2.53, 90°C, 0.17 mV/sec]. It is further assumed that the pH inside the crevice (or pit) is dominated by local hydrolysis reactions, which is assumed to be due to the concentration of $FeCl_3$. Therefore, Table X6 is assumed to apply for Environments A, B and C (see Table 10a for details of assumed environments).

Table 13. Solubilities Given by Pourbaix for Various Compounds Responsible for Passivation of Alloy C-22.

Film Species	$\log(C_1)$	pH_1	$\log(C_2)$	pH_2	m	b	Ref.
$Fe(OH)_2$	-2.5	8	-6.5	10	-2	13.5	Pourbaix p. 311
$Fe(OH)_3$	-1	2	-3	3	-2.00	3.00	Pourbaix p. 311
Fe_2O_3	-1	0	-8	2.5	-2.80	-1.00	Pourbaix p. 311
$Ni(OH)_2$	-1	6.5	-8	10	-2.00	12.00	Pourbaix p. 336
$Cr(OH)_3$	-3	2.5	-12	5.7	-2.81	4.03	Pourbaix p. 268
Cr_2O_3	-3	3.7	-9.5	6	-2.83	7.46	Pourbaix p. 268
$Cr(OH)_3$-nH_2O	0	4	-4	6	-2.00	8.00	Pourbaix p. 268
MoO_3	-3.7	0	1	4.7	1.00	-3.70	Pourbaix p. 276
WO_3	-8	3	0	7	2.00	-14.00	Pourbaix p. 283

Table 14. Predicted Logarithims of Solubilities at Various pH Values – Based on Slopes and Intercepts in Table X1

pH	$Fe(OH)_2$	$Fe(OH)_3$	Fe_2O_3	$Ni(OH)_2$	$Cr(OH)_3$	Cr_2O_3	$Cr(OH)_3$-nH_2O	MoO_3	WO_3
-1	15.50	5.00	1.80	14.00	6.84	10.29	10.00	-4.70	-16.00
0	13.50	3.00	-1.00	12.00	4.03	7.46	8.00	-3.70	-14.00
1	11.50	1.00	-3.80	10.00	1.22	4.63	6.00	-2.70	-12.00
2	9.50	-1.00	-6.60	8.00	-1.59	1.80	4.00	-1.70	-10.00
3	7.50	-3.00	-9.40	6.00	-4.40	-1.03	2.00	-0.70	-8.00
4	5.50	-5.00	-12.20	4.00	-7.21	-3.86	0.00	0.30	-6.00
5	3.50	-7.00	-15.00	2.00	-10.02	-6.69	-2.00	1.30	-4.00
6	1.50	-9.00	-17.80	0.00	-12.83	-9.52	-4.00	2.30	-2.00
7	-0.50	-11.00	-20.60	-2.00	-15.64	-12.35	-6.00	3.30	0.00
8	-2.50	-13.00	-23.40	-4.00	-18.45	-15.18	-8.00	4.30	2.00
9	-4.50	-15.00	-26.20	-6.00	-21.26	-18.01	-10.00	5.30	4.00
10	-6.50	-17.00	-29.00	-8.00	-24.07	-20.84	-12.00	6.30	6.00

Table 15. Alloy Composition Assumed for Congruent Dissolution of Alloy C-22 – Required for Stifling Criterion Calculation

Component	wt. fract.	MW	mol/gram	mol fract. (f_i)
Fe	0.04	55.847	0.000716243	0.043879444
Co	0.02	58.9332	0.000339367	0.020790788
Cr	0.21	51.996	0.004038772	0.24742885
W	0 03	183.85	0.000163177	0.009996745
Mo	0.13	95.94	0.001355014	0.083012714
Ni	0.57	58.7	0.009710392	0.594891456
Total	1			1

Table 16. Maximum Possible Pit Depths (Δx/cm) in Alloy C-22 Predicted with Stifling Criterion of Marsh et al. – Assuming $\Delta C \sim 100\% C_{sat}$ & $i_{pass} \sim 4\ \mu A/cm^2$.

pH	$Fe(OH)_2$	$Fe(OH)_3$	Fe_2O_3	$Ni(OH)_2$	$Cr(OH)_3$	Cr_2O_3	$Cr(OH)_3$-nH_2O	MoO_3	WO_3
-1	$3.48x10^{19}$	$1.65x10^{9}$	$1.04x10^{6}$	$8.11x10^{16}$	$2.02x10^{10}$	$5.70x10^{13}$	$2.92x10^{13}$	**$3.48x10^{-1}$**	**$1.45x10^{-11}$**
0	$3.48x10^{17}$	$1.65x10^{7}$	$1.65x10^{3}$	$8.11x10^{14}$	$3.13x10^{7}$	$8.43x10^{10}$	$2.92x10^{11}$	3.48	**$1.45x10^{-9}$**
1	$3.48x10^{15}$	$1.65x10^{5}$	2.61	$8.11x10^{12}$	$4.85x10^{4}$	$1.25x10^{8}$	$2.92x10^{9}$	$3.48x10^{1}$	**$1.45x10^{-7}$**
2	$3.48x10^{13}$	$1.65x10^{3}$	**$4.14x10^{-3}$**	$8.11x10^{10}$	$7.52x10^{1}$	$1.85x10^{5}$	$2.92x10^{7}$	$3.48x10^{2}$	**$1.45x10^{-5}$**
3	$3.48x10^{11}$	$1.65x10^{1}$	**$6.57x10^{-6}$**	$8.11x10^{8}$	**$1.16x10^{-1}$**	$2.73x10^{2}$	$2.92x10^{5}$	$3.48x10^{3}$	**$1.45x10^{-3}$**
4	$3.48x10^{9}$	**$1.65x10^{-1}$**	**$1.04x10^{-8}$**	$8.11x10^{6}$	**$1.80x10^{-4}$**	**$4.04x10^{-1}$**	$2.92x10^{3}$	$3.48x10^{4}$	**$1.45x10^{-1}$**
5	$3.48x10^{7}$	**$1.65x10^{-3}$**	**$1.65x10^{-11}$**	$8.11x10^{4}$	**$2.79x10^{-7}$**	**$5.97x10^{-4}$**	$2.92x10^{1}$	$3.48x10^{5}$	$1.45x10^{1}$
6	$3.48x10^{5}$	**$1.65x10^{-5}$**	**$2.61x10^{-14}$**	$8.11x10^{2}$	**$4.33x10^{-10}$**	**$8.83x10^{-7}$**	**$2.92x10^{-1}$**	$3.48x10^{6}$	$1.45x10^{3}$
7	$3.48x10^{3}$	**$1.65x10^{-7}$**	**$4.14x10^{-17}$**	8.11	**$6.70x10^{-13}$**	**$1.31x10^{-9}$**	**$2.92x10^{-3}$**	$3.48x10^{7}$	$1.45x10^{5}$
8	$3.48x10^{1}$	**$1.65x10^{-9}$**	**$6.57x10^{-20}$**	**8.11x10-2**	**$1.04x10^{-15}$**	**$1.93x10^{-12}$**	**$2.92x10^{-5}$**	$3.48x10^{8}$	$1.45x10^{7}$
9	**$3.48x10^{-1}$**	**$1.65x10^{-11}$**	**$1.04x10^{-22}$**	**8.11x10-4**	**$1.61x10^{-18}$**	**$2.86x10^{-15}$**	**$2.92x10^{-7}$**	$3.48x10^{9}$	$1.45x10^{9}$
10	**$3.48x10^{-3}$**	**$1.65x10^{-13}$**	**$1.65x10^{-25}$**	**8.11x10-6**	**$2.49x10^{-21}$**	**$4.23x10^{-18}$**	**$2.92x10^{-9}$**	$3.48x10^{10}$	$1.45x10^{11}$

Note: Ranges of pH where localized corrosion is stiffled by a particular film-forming compound are in bold-face type. At low pH, MoO_3 and WO_3 appear to be primarily responsible for the superior corrosion performance of Alloy C-22. Localized corrosion should be stiffled over the entire range of pH, extending from –1 to 10. This is consistent with observation in most (but not all) acidic media.

Table 17. Maximum Possible Pit Depths (Δx/cm) in Alloy C-22 Predicted with Stifling Criterion of Marsh et al. – Assuming $\Delta C \sim 10\% C_{sat}$ & $i_{pass} \sim 4\ \mu A/cm^2$.

pH	$Fe(OH)_2$	$Fe(OH)_3$	Fe_2O_3	$Ni(OH)_2$	$Cr(OH)_3$	Cr_2O_3	$Cr(OH)_3$-nH_2O	MoO_3	WO_3
-1	$3.48x10^{18}$	$1.65x10^{8}$	$1.04x10^{5}$	$8.11x10^{15}$	$2.02x10^{9}$	$5.70x10^{12}$	$2.92x10^{12}$	**$3.48x10^{-2}$**	**$1.45x10^{-12}$**
0	$3.48x10^{16}$	$1.65x10^{6}$	$1.65x10^{2}$	$8.11x10^{13}$	$3.13x10^{6}$	$8.43x10^{9}$	$2.92x10^{10}$	**$3.48x10^{-1}$**	**$1.45x10^{-10}$**
1	$3.48x10^{14}$	$1.65x10^{4}$	**$2.61x10^{-1}$**	$8.11x10^{11}$	$4.85x10^{3}$	$1.25x10^{7}$	$2.92x10^{8}$	3.48	**$1.45x10^{-8}$**
2	$3.48x10^{12}$	$1.65x10^{2}$	**$4.14x10^{-4}$**	$8.11x10^{9}$	7.52	$1.85x10^{4}$	$2.92x10^{6}$	$3.48x10^{1}$	**$1.45x10^{-6}$**
3	$3.48x10^{10}$	**1.65**	**$6.57x10^{-7}$**	$8.11x10^{7}$	**$1.16x10^{-2}$**	$2.73x10^{1}$	$2.92x10^{4}$	$3.48x10^{2}$	**$1.45x10^{-4}$**
4	$3.48x10^{8}$	**$1.65x10^{-2}$**	**$1.04x10^{-9}$**	$8.11x10^{5}$	**$1.80x10^{-5}$**	**$4.04x10^{-2}$**	$2.92x10^{2}$	$3.48x10^{3}$	**$1.45x10^{-2}$**
5	$3.48x10^{6}$	**$1.65x10^{-4}$**	**$1.65x10^{-12}$**	$8.11x10^{3}$	**$2.79x10^{-8}$**	**$5.97x10^{-5}$**	2.92	$3.48x10^{4}$	**1.45**
6	$3.48x10^{4}$	**$1.65x10^{-6}$**	**$2.61x10^{-15}$**	$8.11x10^{1}$	**$4.33x10^{-11}$**	**$8.83x10^{-8}$**	**$2.92x10^{-2}$**	$3.48x10^{5}$	$1.45x10^{2}$
7	$3.48x10^{2}$	**$1.65x10^{-8}$**	**$4.14x10^{-18}$**	**$8.11x10^{-1}$**	**$6.70x10^{-14}$**	**$1.31x10^{-10}$**	**$2.92x10^{-4}$**	$3.48x10^{6}$	$1.45x10^{4}$
8	3.48	**$1.65x10^{-10}$**	**$6.57x10^{-21}$**	**$8.11x10^{-3}$**	**$1.04x10^{-16}$**	**$1.93x10^{-13}$**	**$2.92x10^{-6}$**	$3.48x10^{7}$	$1.45x10^{6}$
9	**$3.48x10^{-2}$**	**$1.65x10^{-12}$**	**$1.04x10^{-23}$**	**$8.11x10^{-5}$**	**$1.61x10^{-19}$**	**$2.86x10^{-16}$**	**$2.92x10^{-8}$**	$3.48x10^{8}$	$1.45x10^{8}$
10	**$3.48x10^{-4}$**	**$1.65x10^{-14}$**	**$1.65x10^{-26}$**	**$8.11x10^{-7}$**	**$2.49x10^{-22}$**	**$4.23x10^{-19}$**	**$2.92x10^{-10}$**	$3.48x10^{9}$	$1.45x10^{10}$

Note: Ranges of pH where localized corrosion is stiffled by a particular film-forming compound are in bold-face type. At low pH, MoO_3 and WO_3 appear to be primarily responsible for the superior corrosion performance of Alloy C-22. Localized corrosion should be stiffled over the entire range of pH, extending from –1 to 10. This is consistent with observation in most (but not all) acidic media.

Table 18. Penetration Rates for Localized Corrosion of Alloy C-22, Estimated to Account for the Stifling Effect – 50th Percentile Based on Multivariable Linear Regression Analysis of 6-Month Data from LTCTF, Published Haynes Data (Asphahani), and Converted Corrosion Currents from Cyclic Polarization (Roy).

J-13 Concentration	1000X	1000X	1000X	Saturated	Saturated	Saturated
T(°C)	25	50	100	25	50	100
NaCl (wt.%)	1.2	1.2	1.2	1.2	1.2	1.2
$FeCl_3$ (wt.%)	1	1	1	10	10	10
pH (crevice or pit)	1.92	1.92	1.92	0.7	0.7	0.7
	microns/yr	microns/yr	microns/yr	microns/yr	microns/yr	microns/yr
Percentile = 50%	3.58×10^{-3}	7.67×10^{-3}	7.70×10^{-2}	2.48	10.50	105.44
	microns/yr	microns/yr	microns/yr	microns/yr	microns/yr	microns/yr
Percentile = 5%	2.76×10^{-4}	5.89×10^{-4}	5.92×10^{-3}	0.19	0.81	8.11
	microns/yr	microns/yr	microns/yr	microns/yr	microns/yr	microns/yr
Percentile = 95%	4.66×10^{-2}	9.97×10^{-2}	1.00	32.24	136.57	1371.66
	microns/yr	microns/yr	microns/yr	microns/yr	microns/yr	microns/yr
Percentile = 1%	8.75×10^{-5}	1.87×10^{-4}	1.88×10^{-3}	0.06	0.26	2.57
	microns/yr	microns/yr	microns/yr	microns/yr	microns/yr	microns/yr
Percentile = 99%	3.23×10^{-1}	6.90×10^{-1}	6.93	223.06	945.03	9491.35

Note: correlation accurately predicts 1 year observations within the bounds of experimental measurements.

Probability of Environment A, B and C.

The following probabilities are assumed regarding Environments A, B and C: Environment A (340 mV vs. SHE, pH 2.5) = 45%; Environment B (640 mV vs. SHE, pH 2.5) = 10%; Environment C (340 mV vs. SHE, pH 5-7) = 45%. As shown in Table 9b, an open circuit potential of 714 mV vs. SHE has been observed with Alloy C-22 in 3.05 wt. % $FeCl_3$ at 90°C. However, it is believed that most sites will experience more milder conditions. In the opinion of this member of the EEP, the largest source of uncertainty in corrosion modeling is the unspecified (unknown) waste package environment.

Recommendations

1. Continuity of EEP. Continued involvement of members of Expert Elicitation Panel (EEP) members from outside of Yucca Mountain Program. For continuity, this member believes that the EEP should maintain involvement in conceptual model development, providing the types of guidance that has resulted from this process. This will provide the advantage of eliminating any possible time delay (and associated costs) required to educate a new EEP on issues specifically related to repository design and construction.

2. Technical Guidance. Specific expertise of members of the EEP should be exploited by the program to enhance experimental and predictive strategies.

   Guidance on Stress Corrosion Cracking. Dr. Andresen should be heavily involved in planning activities regarding stress corrosion cracking of both the CAM and CRM. Dr. Andresen in an international authority on the subject and has developed predictive capability in this technical area that is now relied upon by the nuclear power industry. Preliminary estimates by Dr. Jia-Song Huang indicate that a pre-existing flaw of 1.2-1.4 cm near a weld might give rise to SCC [Jia-Song Huang, "Stress Corrosion Cracking in Canistered Waste Package Containers: Welds

and Base Metals" and "Thermal Embrittlement of Carbon Steels in Canistered Disposal Containers," in Memorandum entitled "Stress Corrosion Cracking and Thermal Embrittlement in Waste Packages," Lawrence Livermore National Laboratory, Memorandum, September 25, 1997, 9 pages]. The possibility of having such a flaw and the impact on container life should be further investigated. A wide variety of valuable SCC tests are now being conducted at LLNL by Dr. Ajit Roy. These tests employ a variety of experimental techniques, including slow strain rate testing. Other techniques, such as the reverse-dc approach used by General Electric may also be of value for measuring crack propagation rates at low stress intensity. LLNL has a custom instrument that was obtained from General Electric for making such measurements. The possibility of employing this instrument at LLNL or at another designated facility should be explored in collaboration with Drs. Andresen and Roy. The possibility of using acoustic emission with guard sensors should be explored again, as it was by this EEP member during the late 1980's.

Pitting and Localized Corrosion. The expertise of Prof. Scully and his unique experimental capability for elucidating pit initiation and propagation phenomena should be exploited to support the development of mechanistic pitting models (models based upon stochastic probability theory) capable of accurate quantitative predictions. The proper dependence of rate expressions on temperature, potential, pH, and anion concentration must be established. Parameters must then be quantified. Specific rates of interest include those for: birth and death of embryos; embryo conversion to stable pits; penetration; and stifling (or a verifiable quantitative criterion). Techniques such as electrochemical noise analysis need to be implemented, along with microscopic evaluation. Both the CAM and CRM should be investigated.

3. Passive Film Stability on CRM. Detailed studies of the passive film formed on Alloy C-22 should be performed, establishing stability in various environments. This very thin film (tens of Angstroms) is key to waste package survival and requires atomic resolution for imaging defects. The STM provides a picture of the atomic arrangement of a surface by sensing corrugations in the electron density of the surface that arise from the positions of surface atoms ["Scanning Tunneling Microscopy: Opening a New Era of Materials Engineering," Science and Technology Review, Lawrence Livermore National Laboratory, August, 1995, pp. 4-11]. A finely sharpened tungsten wire (or tip) is first positioned within 20 Angstroms of the specimen by a piezoelectric transducer, a ceramic positioning device that expands or contracts in response to a change in applied voltage. This arrangement enables us to control the motion of the tip with subnanometer precision. At this small separation, as explained by the principles of quantum mechanics, electrons tunnel through the gap, the region of vacuum between the tip and the sample. If a small voltage (bias) is applied between the tip and the sample, then a net current of electrons (the tunneling current) flows through the vacuum gap in the direction of the bias. For a suitably sharpened tip, one that terminates ideally in a single atom, the funneling current is confined laterally to a radius of a few tenths of a nanometer. The remarkable spatial resolution of the STM derives from this lateral confinement of the current. Next, additional piezoelectric transducers are used to raster the tip across a small region of the sample. As the tip scans the surface, corrugations in the electron density at the surface of the sample cause corresponding variation in the tunneling current. By detecting the very fine changes in tunneling current as the tip is swept across the surface, we can derive a two-dimensional map of the corrugations in electron density at the surface [J. Golovchenko, " The Tunneling Microscope: A New Look at the Atomic World," Science, Vol. 232, 1986, p. 48]. Potentials below and above the critical pitting potential should be explored. It is believed that such studies will enable investigators to establish the critical pitting potential and threshold chloride

concentration with a higher degree of confidence than possible with cyclic polarization [R. D. McCright, J. C. Farmer, D. L. Fleming, "An Electrochemical Approach to Predicting Corrosion Performance of Container Materials," Proceedings of the 2nd Annual International High-Level Radioactive Waste Management Conference and Exposition, Las Vegas, NV, Apr. 28 - May 3, 1991, American Nuclear Society and American Society of Civil Engineers, Vol. 2, 1991, pp. 940-944]. More specifically, anion adsorption and pit initiation can be observed with atomic resolution in real time. In addition to observing pit embryos formed from halide nuclei, the STM probe could also be used to induce pits. Subsequently, the process of repassivation (healing of the passive film) can be investigated. Defects in the passive film believed to be pit embryos will be imaged. After exposure, the samples should be rinsed, dried and transferred to UHV for further inspection with both STM and complimentary techniques. A unique capability has been developed at LLNL which includes STM, low-energy electron diffraction (LEED), and other surface diagnostics in an ultra-high vacuum (UHV) chamber. The LEED capability enables determination of long-range order, while the STM provides information about short-range order. This combination of surface diagnostics has been used to study the structural development of thin films (films from one atom to several hundreds of Angstroms thick) during vapor deposition on single-crystal substrates. For example, the deposition of molybdenum atoms on atomically clean silicon has been investigated [P. Bedrossian, "One-Dimensional Ordering at the Mo/Si Interface," Surface Science, Vol. 320, 1994, p. 247; "Nucleation and Ordering of $MoSi_2$ on Si(100)," Surface Science, Vol. 322, 1995, p. 73]. Transmission electron microscopy (TEM) can also be employed to study cross-sections of atomically thin films, as has been done with multilayer semiconductor films deposited by magnetron sputtering [J. C. Farmer et al., "Sputter Deposition of Multilayer Thermoelectric Films: An Approach to the Fabrication of Two-Dimensional Quantum Wells," Thirteenth International Conference on Thermoelectrics, Kansas City, Missouri, August 30 to September 1, 1994, American Institute of Physics Proceedings 316, Eds. Mathiprakasam, B., Heenan, P., American Institute of Physics Press, New York, NY, 1994, pp. 217-225]. Experiments to establish the integrity of the passive film on Alloy C-22 are of crucial importance to TSPA and is essential for validation of the conceptual model discussed here.

4. Microsensors and in situ optical techniques should be employed to actually measure the localized environment inside the CAM-CRM crevice. Fiber optic microprobes (fluorescence, absorption, and inelastic Raman scattering) should be used to determine pH, as well as the concentrations of dissolved metals and anions. Microelectrodes should be used to establish potential profiles within the crevice. Such measurements will eliminate much of the need for speculation about the crevice environment. Such sensors have already been demonstrated at LLNL and will be applied to this important problem in the future, provided that funding is maintained. In specific regard to Alloy C-22, it may be possible to use interferometry and other reflection techniques (ellipsometry, etc.) to quantify the very small penetration rates anticipated in crevices. For example, an artificial crevice could be formed beneath a quartz optical window, with $FeCl_3$ additions to simulate the dissolved CAM.

5. Thin-film corrosion sensors should be fabricated and deployed in the drifts at Yucca Mountain (ESF) to continuously monitor corrosion rates of A516 Gr. 12, Alloy C-22, and other metallic alloys of interest. Such films can be deposited on piezoelectric crystals so that mass change due to corrosion can be measured. Alternatively, the resistance through a sputtered thin film of the material can also be monitored. Such atmospheric corrosion studies are now being conducted at LLNL to study the impact of various gas-phase impurities on the tarnish rate of unprotected metallic mirrors in the National Ignition Facility. Phase stability could be studied with sputtered multilayers (well defined, calibrated microstructure).

6. Process-level (mechanistic) models for pitting and crevice corrosion should be further developed and improved so that experimental data can be used for reliable predictions on the repository time frame. The CAM-CRM crevice transport model should be enhanced to include: (a) localized concentration- and temperature-dependent solution conductivity; (b) terms to account for electromigration at low ionic strengths; (b) equations to account for sulfate, nitrate, carbonate, and other anions; (c) an appropritate activity coefficient model; (d) improved computationally-efficient model of solution equilibria, including proper hydrolysis equilibrium constants; (e) ability to deal with variable width crevice; (f) ability to account for localized breakdown of the passive film within the crevice; and (g) a rigorous criterion for cessation of localized attack. Improvements are also needed in the stochastic pitting model, as previously discussed. These specific comments reflect noted recommendations of Prof. Joseph Payer [Case Western Reserve University], Prof. Denny Jones [University of Nevada, Reno], Dr. Narsi Sridar [Center forNuclear Waste Regulatory Analysis, San Antonio], Dr. Kevin McCoy [Framatome Cogema Fuels, Las Vegas], and others.

7. A full-time professional statistician with a background in physics, chemistry and engineering is need to be involved in the continuous evaluation and correlation of the large volumes of data now being generated by the Long Term Corrosion Test Facility at LLNL. The correlation presented in this elicitation report is viewed as a starting point, and requires continuous improvement and updating. More appropriate, non-linear functional forms should be explored. Such functional forms will enable TSPA to interpret coefficients as activation energies, orders of reaction, and related kinetic parameters. Modification of the existing test matrix should be considered. By adding additional test conditions as needed (tanks), it may be possible to achieve the advantages of a factorial design. Members of the EEP should be updated on revisions in correlations.

8. All cyclic polarization measurements should be accompanied by microscopic photographs, and perhaps even images generated by a scanning electron microscope (SEM), to substantiate the absence of localized corrosion below threshold potentials (repassivation potential, etc.). This approach has been successfully employed with great success by Dr. Gustavo Cragnolino [G. A. Cragnolino, DOE/NRC Appendix 7 Meeting, Livermore, CA, February, 1998], and should be emulated by LLNL. As recommended by Dr. Andresen, all electrochemical potential measurements should be presented with a conversion to the standard hydrogen electrode (SHE) scale to facilitate comparison with the Pourbaix diagram and other data sources.

9. It is believed that uncertainty regarding the waste package environment is the largest source of uncertainty on corrosion modeling. Significant effort must be expended by the entire program to reduce this uncertainty, and to provide those involved in TSPA and materials testing with well-specified anticipated environments.

Technical Information Department • **Lawrence Livermore National Laboratory**
University of California • Livermore, California 94551